

I.

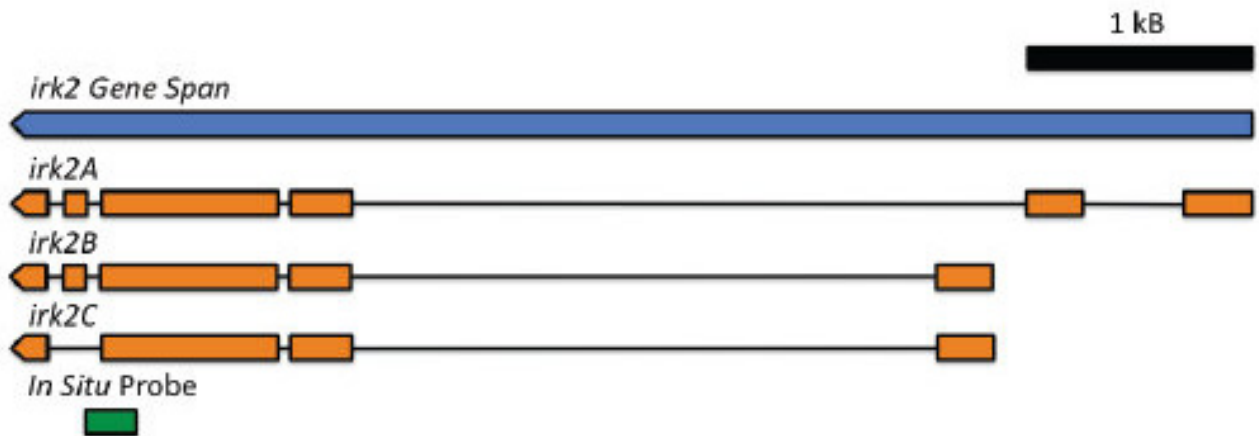


Fig. S1. *irk2* expression. (A-H) In situ with *irk2* sense (A,B,D) and *irk2* antisense (C,E-H) probes showing expression of *irk2* in the third instar larval imaginal wing disc (A,E), larval trachea (B,F), embryonic trachea and mouthhooks (C,D,G,H). We assayed for the presence of *irk2* mRNA transcripts in the embryo, the imaginal discs and other larval structures by in situ hybridization. An *irk2* antisense probe revealed that *irk2* is expressed in the *Drosophila* wing disc. *irk2* is also expressed in the embryonic larval trachea, mouth hooks and tracheal branches. (I) The location of the in situ probe is shown in a schematic.

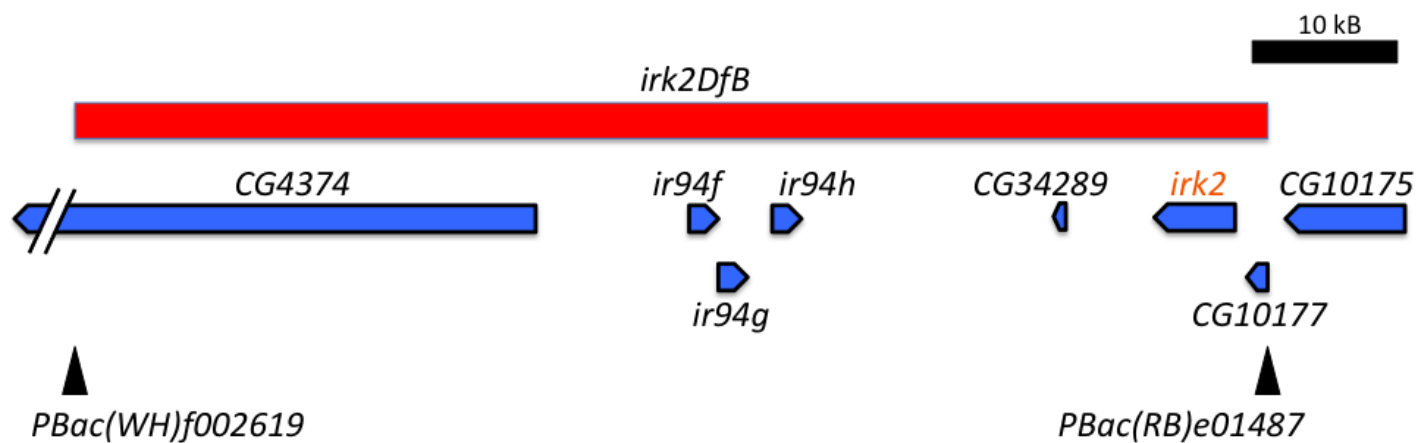


Fig. S2. Map of genomic region including *irk2* showing the start and end points of each deficiency (*irk2Df A* and *irk2Df B*).

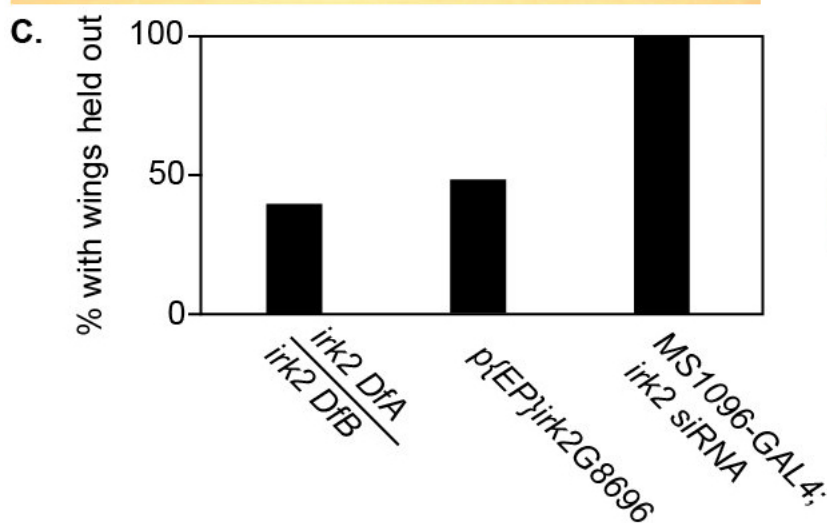
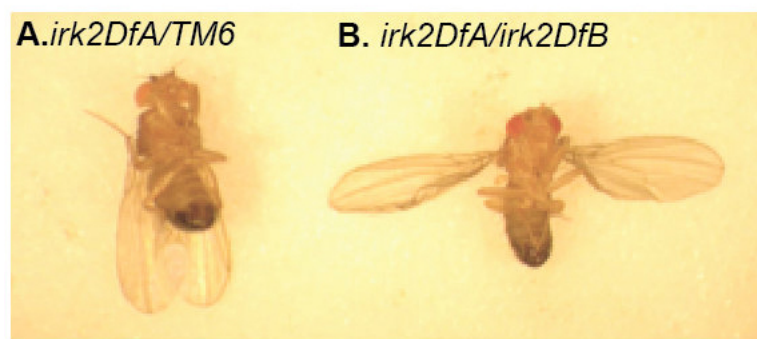


Fig. S3. Reducing function of *irk2* causes hinge defects similar to the Dpp ‘wings held-out’ phenotype. (A) Heterozygous *irk2Df/+* with wild-type wing hinge. (B) The wings held out phenotype of *irk2DfA/irk2DfB* male fly. (C) Graph showing prevalence of the wings held out phenotype for the *irk2DfA/irk2DfB* MS1096-GAL4 *irk2* siRNA. (D) Side view of the hinge defect that results in the wings held-out phenotype of a MS1096-GAL4 *irk2* siRNA male fly.

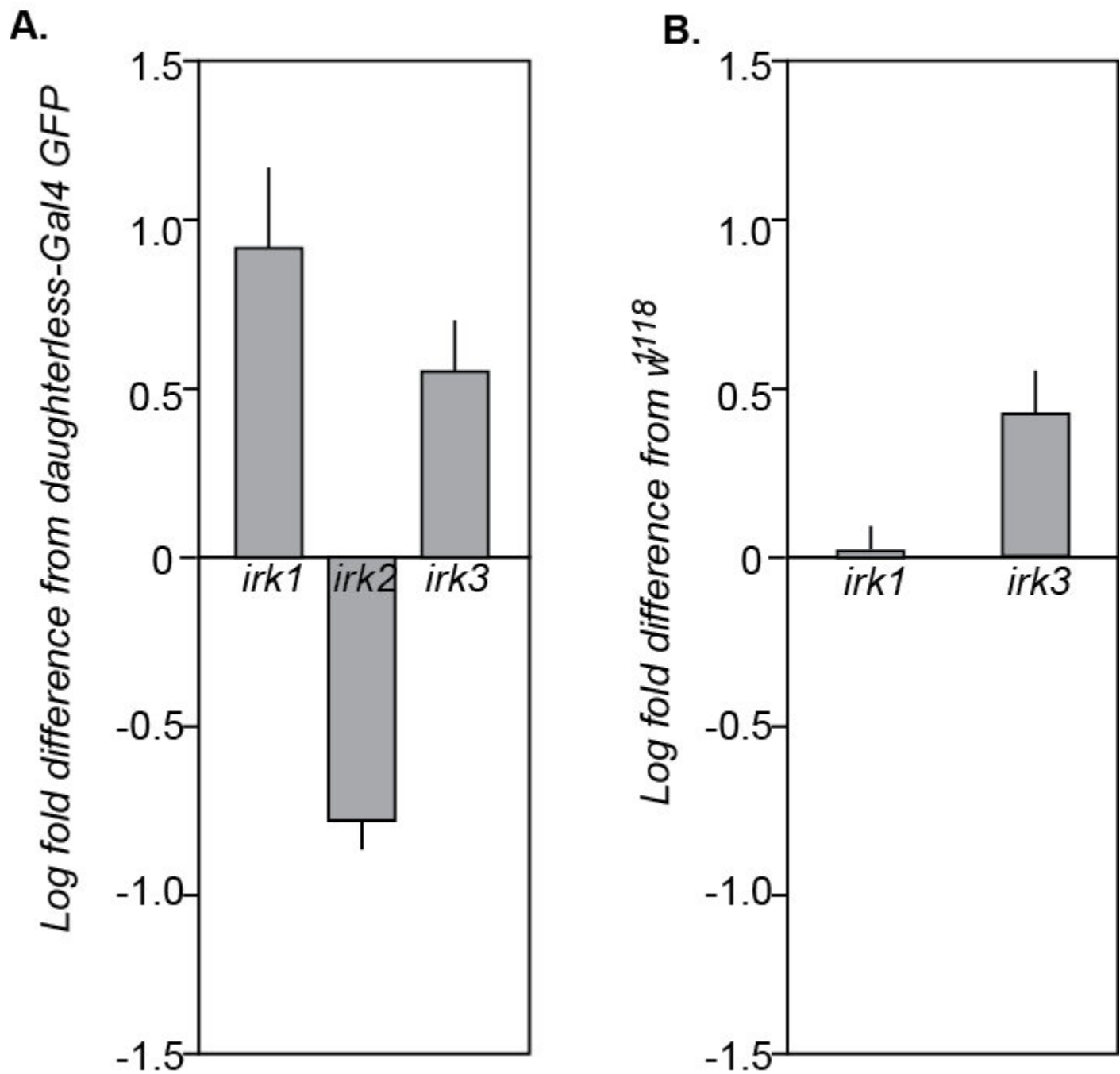


Fig. S4. Reducing function of *irk2* increases expression of other *irk* subunits. Quantitative RT PCR of *irk1*, *irk2* and *irk3* transcripts isolated from *daughterless-GAL4 irk2 siRNA* compared with *daughterless-GAL4 GFP* (A) and *irk1*, and *irk3* transcripts from *irk2DfA/irk2DfB* compared with Berlin w^{1118} . Error bars represent s.e.m. Graph represents five independent experiments (B).

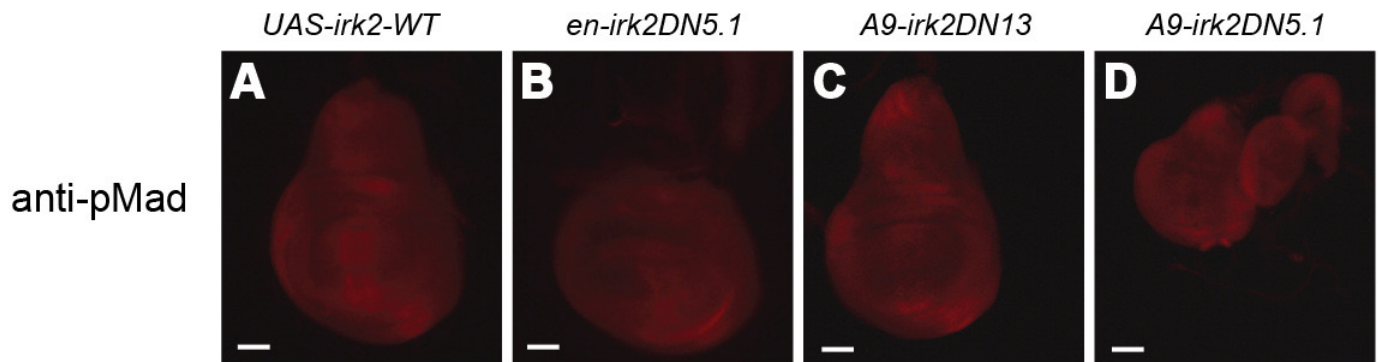


Fig. S5. Expression of *irk2DN* using wing-directed Gal4 drivers decreases anti-p-Mad staining. Wing discs of third instar larva stained with Anti-phospho-Smad 1/5 antibody (A) *en-Gal4; UAS-irk2WT*. (B) *A9-Gal4; UAS-irk2DN13*. (C) *A9- UAS-irk2DN5.1*